A Strategy to Enhance the Distribution Systems Recoverability via the Simultaneous Coordination of Planning Actions and Operational Resources

Juan M. Home-Ortiz[1*], Ozy D. Melgar-Dominguez[1], Mohammad Sadegh Javadi[2], Matthew B Gough[2], José Roberto Sanches Mantovani[1], and João P. S. Catalão [2]

[1] Electrical Engineering Department, São Paulo State University (UNESP), Ilha Solteira, São Paulo, Brazil. (emails:{juanmanuelhome, ozzydamedo}@gmail.com, mant@dee.feis.unesp.br)

[2] Faculty of Engineering of the University of Porto and INESC TEC, Porto. Portugal (e-mail: catalao@fe.up.pt)

[*] Corresponding Author, Av. Brasil 056, UNESP - Campus de Ilha Solteira, Departamento de Engenharia Elétrica, Ilha Solteira, 15385000, São Paulo, Brazil. Tel: 3743-1000.

Abstract

This paper presents a planning and operational strategy to improve the recoverability of distribution systems (DSs) to deal with a set of possible line fault scenarios. The strategy simultaneously optimizes the allocation of dispatchable distributed generation (DG) units while coordinating a dynamic restoration process based on a radial topology reconfiguration, an islanding operation, a demand response program, and the pre-positioning and dispatch of mobile emergency storage units. The uncertainty and variability associated with solar irradiation and demand are captured via a multi-period formulation based on a stochastic mixed-integer linear programming model. The objective function of this model minimizes the investment cost of new dispatchable DG units and the amount of energy shedding within the system. Simulations are performed on adapted 33-node and 53-node test systems to validate the proposed strategy under four different test conditions, numerical results reveal the advantages of simultaneously solving the planning and operational stages to improve the recoverability of the system.

Keywords: Demand response, distributed generation allocation, distribution systems, mobile emergency storage, resilience, restoration.

Nomenclature

Sets

Γ_S Set of nodes with substation

Γ_G^N Set of candidate nodes to install dispatchable DG

Γ_B/Γ_N Set of real branches / nodes of the system

$\Gamma_N^{mes}/\Gamma_{st}$ Set of connection nodes for MES / staging location

$\Gamma_C^t/\Gamma_T/\Gamma_F$ Set of stochastic scenarios/ time period/ fault events

$\Gamma_{\overline{n}}^{mes}$ Set of maximum MES units to be pre-positioned

Γ_B^* Set real and fictitious branches with indexes ij and ji

Γ_B^h Set of fictitious branches

Γ_G Set of nodes with a dispatchable DG

Γ_N^f Set of nodes that were not affected by the fault scenarios

Γ_P Set nodes with a PV-based generation unit

Parameters

δ_i Demand response program limit

Δ_t Duration of a time period

ϕ^{pv} Power generation factor of the PV-based units

$\rho_{t,c}$ Probability of stochastic scenario

$\sigma_i^{dg/ls}$ Investment DG / Load shedding cost

$\xi_{i,t,c}$ PV generation level

C_i^t Required time to connect a MES unit at node i

$\overline{I}_{ij}$ Current power limit of a line

P^d/Q^d Active/reactive power demand

$P^{pv}_{i,t,c}$ PV generation capacity available

R_{ij}/X_{ij} Resistance/reactance of a branch

$\overline{S}^{dg/ss}_{i}$ Apparent power limit of DG / substation

$T^{cf}_{st,i}$ Time considered to be affected by the road congestion between a staging location and a node

$T^{t}_{st,i}$ Traveling time from a staging location to a node

$\overline{V}$, $\underline{V}$ Maximum/minimum voltage limits

Binary variables

$h_{ij,t,f}$ Binary variable to determine the radiality of the grid

$e_{i,t,c,f}$ Binary variable that indicates the operational state of a MES unit

g_i Binary variable that defines the investment on a new dispatchable DG

$k^{mes}_{st,n}$ Binary variable that defines the pre-positioned MES units at a staging location

$u_{i,n,t,f}$ Binary variable that defines the n MES units connected at a node

$w_{i,n,t,f}$ Binary variable that defines the connection period of a MES unit at a node

$x_{i,t,f}$ Binary variable for operational state of a node

$y_{ij,t,f}$ Binary variable for operational state of a branch

$z^{mes}_{st,i,n,f}$ Binary variable that indicates the displacement of n MES units from a staging location to a node

Continuous variables

$\ell^{sqr}_{ij,t,c,f}$ Square of the current

$b^{v/g}_{ij,t,c,f}$ Slack variable for voltage calculation

$p^{dg/ss}_{i,t,c,f}$ Active power injected by DG / substation

$p^{dr}_{i,t,c,f}$ Active power demand considering DR program

$p^{ndg}_{i,t,c,f}$ Active power injected by a new installed DG

$p_{ij,t,c,f}$ Active power flow through a line.

$p^{mesch}_{i,t,c,f}$ Active power charging by a MES unit

$p^{mesd}_{i,t,c,f}$ Active power discharging by a MES unit

$p^{pv}_{i,t,c,f}$ Active power injected by a PV unit

$q^{dr}_{i,t,c,f}$ Reactive power demand considering DR program

$q^{dg/ss}_{i,t,c,f}$ Reactive power injected by DG / substation

$q^{ndg}_{i,t,c,f}$ Active power injected by a new installed DG

$q^{pv}_{i,t,c,f}$ Reactive power injected by a PV unit

$q_{ij,t,c,f}$ Reactive power flow through a line

$\tau^{x}_{st,i,n,f}$ Traveling time by n MES units from a staging location to a node

$soc^{mes}_{i,t,c,f}$ State of charge of a MES unit connected at a node

$v^{sqr}_{i,t,c,f}$ Square of the voltage.

1. Introduction

The solution to the expansion planning problem in distribution systems (DSs) seeks to provide an effective investment plan that leads to a safe and reliable energy service to active and passive users. Due to the mathematical complexity that involves an expansion planning problem, it is commonly formulated considering only normal operating conditions, without taking into account the occurrence of extreme fault events. An approach based on resilience analysis requires the development of more robust planning strategies to improve the efficiency and recoverability of a DS against emergency conditions. In this regard, it is necessary to enhance the traditional perspective of the current planning methodologies, giving rise to more sophisticated strategies to design resilient systems [1], [2].

Inherently, the process of improving the DS resilience can be achieved through optimal coordination of operational resources. For example, [3] and [4] propose the coordination of switching operations to reallocate the out-of-service nodes of the system to auxiliary feeders, assessing passive and active DS, respectively. When distributed generation (DG) units are placed in the system, the restoration process allows for the formation of microgrids to improve the DS recoverability [5]. In this research field, the authors in [6] propose a strategy to improve the recoverability of the system via an islanding operation with a master-slave DG scheme, where large DG units operate as master units at the reference node of a microgrid, while renewable and small DG

units are operated as slave units. In [7], the on-outage portion of the DS is sectionalized into microgrids, and the power dispatch of existing DG units is re-dispatched to supply affected users. As an alternative approach to improve the service restoration process, reference [8] proposes the optimal coordination of energy storage devices considering microgrid formation.

As new trends to deal with the occurrences of fault events, mobile energy sources are incorporated in the design of modern DSs due to their flexibility and rapid connection close to the fault locations in the system [9]. In this regard, a restoration strategy to co-optimizes the operation of mobile power sources and repair crews is presented in [10], where the main objective consists of maximizing the service time of critical loads. Similarly, in the approach developed by the authors in [11], it is simultaneously coordinated the optimal dispatch of mobile emergency generators (MEGs) and repair crews with the dynamic microgrid formation in order to maximize, as much as possible, the amount of demand in-service after the occurrence of a fault event. In the same research field, another approach is presented in reference [12], where the authors investigate the optimally pre-location MEGs and repair crews to prepare, in advance, the DS to face a set of possible high-impact fault events. In addition, as another alternative to deal with emergency conditions, mobile energy storage systems (MESs) arise as modern resources that can provide a backup option in order to enhance the DS resilience. Nowadays, several approaches have been developed to simultaneously incorporate this alternative with dynamic microgrid formation. Consequently, more robust resilience-based strategies are designed [13]-[14].

On the other hand, demand response (DR) programs have been exploited as an additional operational resource to improve the system's operation by modifying demand behavior and, as a consequence, increasing the system's flexibility [15]. These DR programs have significant advantages that can be explored simultaneously with other alternatives to enhance the system resilience, maximizing the in-service load after a restoration process [16], [17], [18]. For example, in [18] is investigated the benefits by incorporating a DR program in the restoration process which is co-optimized with alternatives as mobile resources to increase the amount of recovered energy after the occurrence of a high-impact fault event.

Notwithstanding, when the implementation of operational resources to improve the DS resilience is exhausted, some investment actions could be necessary for hardening DSs in order to mitigate the negative impacts due to high-impact fault events [19]. To do so, some approaches have investigated the optimal allocation of dispatchable DGs with microgrid formation in radial and meshed topologies [20], DG allocation with microgrid formation with master-slave DG operation [21], line hardening and backup generator allocation simultaneously optimized with network reconfiguration and microgrid formation [22], assessment of photovoltaic hosting capacity under normal and emergency conditions by implementing planning and operational

actions to improve the DS recoverability [23].

Although there is a significant number of approaches to deal with high-impact fault events in both the planning and operation stages of a DS, there is a gap in the formulation of the DS resilience problem, where the stages of planning and operation are rarely approached in the problem formulation. To fill the existing void, the proposed work seeks to approach the DS resilience problem through a planning and operational strategy that incorporates the DG allocation problem with the coordination of several operational resources, such as a demand response program and the optimal pre-positioning and dispatch of MESs. It is important to highlight that in contrast with the existing literature, the proposed work presents significant contributions that are categorized as follows:

- From the distribution system operator's point of view, it is proposed a novel strategy designed to simultaneously capture expansion planning and operational decisions to deal with emergency conditions due to the occurrence of high-impact fault events. The developed strategy seeks to improve the restoration process in radial distribution systems by the co-optimization of DG allocation with the coordination of operational resources such as dynamic switching operations, dispatch of MESs units, islanding operation, and the incorporation of a demand response program.

- Formulating the DS resilience problem via a multi-period stochastic approach based on a solver-friendly mixed-integer linear programming model. This mathematical formulation is a support tool that could assist the DS planner in the decision-making process to obtain more resilient and robust DSs capable of facing high-impact fault events.

The remainder of this paper is organized as follows: Section 2 presents the mixed-integer linear programming (MILP) model of the problem; numerical results considering a 33-node distribution system and discussion are presented in Section 3; finally, Section 4 presents the conclusions drawn from this paper.

2. Problem and Mathematical Formulation

The presented work proposes a strategy that simultaneously involves the planning and operation stages. In the planning stage, the optimal location and capacity for new connections of dispatchable DG units are derived. Meanwhile, in the operation stage, the expected amount of out-of-service load of the system after a set of high-impact fault events is minimized. This stage uses coordinated operational resources such as a dynamic restoration scheme with switching operations, the pre-positioning and dispatching of MES units, and a demand response program. A MILP multi-period stochastic formulation is proposed to solve this problem because commercial optimization solvers can tackle this kind of model, guaranteeing a finite solution to the

problem. Therefore, this section formulates this problem as a single-objective stochastic MILP model as follows:

2.1. Objective function

The objective function (1) minimizes the investment cost of new dispatchable DG units and the expectation of out-of-service load over a set of fault scenarios and demand uncertainties.

$$\min \sum_{i\in\Gamma_G^n} \sigma_i^{dg} g_i + \sum_{t\in\Gamma_T}\sum_{c\in\Gamma_C^t}\sum_{f\in\Gamma_F}\left[\rho_{t,c}\sum_{i\in\Gamma_N}\sigma_i^{ls}\Delta_t P_{i,t,c}^{d} x_{i,t,f}\right] \tag{1}$$

The investment cost of new dispatchable DG units is defined according to the status of the binary variable g_i, which belongs to the first stage of the two-stage stochastic formulation since it does not depend on the uncertainties of the problem. The second term determines the load-shedding cost considering the nodes that cannot be restored during the dynamic restoration process. For each fault scenario f, if node i is in-service, then $x_{i,t,f} = 0$, otherwise if node i is out-of-service, then $x_{i,t,f} = 1$. In this regard, $x_{i,t,f}$ is a stochastic scenario-dependent variable, and as such, it belongs to the second stage of the two-stage stochastic formulation.

2.2. Operational constraints

The operating state of an DS for each fault scenario is determined by the set of constraints (2)-(6), where the indices i, ij, t, c, f correspond to the sets $\Gamma_N, \Gamma_B, \Gamma_T, \Gamma_C^t, \Gamma_F$, respectively.

$$\begin{aligned}
&\sum_{ji\in\Gamma_B} p_{ji,t,c,f} - \sum_{ij\in\Gamma_B}(p_{ij,t,c,f} + R_{ij}\ell_{ij,t,c,f}^{sqr}) + p_{i,t,c,f}^{ss} + \\
&p_{i,t,c,f}^{pv} + p_{i,t,c,f}^{dg} + p_{i,t,c,f}^{ndg} + p_{i,t,c,f}^{mesd} = p_{i,t,c,f}^{dr} + p_{i,t,c,f}^{mesch}, && \forall(i,t,c,f), && (2)\\
&\sum_{ji\in\Gamma_B} q_{ji,t,c,f} - \sum_{ij\in\Gamma_B}(q_{ij,t,c,f} + X_{ij}\ell_{ij,t,c,f}^{sqr}) + q_{i,t,c,f}^{ss} + \\
&\quad q_{i,t,c,f}^{pv} + q_{i,t,c,f}^{dg} + q_{i,t,c,f}^{ndg} = q_{i,t,c,f}^{dr}, && \forall(i,t,c,f), && (3)\\
&v_{i,t,c,f}^{sqr} - v_{j,t,c,f}^{sqr} + b_{ij,t,c,f}^{v} = 2(R_{ij}p_{ij,t,c,f} + X_{ij}q_{ij,t,c,f}) + \ell_{ij,t,c,f}^{sqr} Z_{ij}^2, && \forall(ij,t,c,f), && (4)\\
&-(\overline{V}^2 - \underline{V}^2)(1 - y_{ij,t,f}) \le b_{ij,t,c,f}^{v} \le (\overline{V}^2 - \underline{V}^2)(1 - y_{ij,t,f}), && \forall(ij,t,c,f), && (5)\\
&v_{j,t,c,f}^{sqr}\ell_{ij,t,c,f}^{sqr} = p_{ij,t,c,f}^2 + q_{ij,t,c,f}^2, && \forall(ij,t,c,f). && (6)
\end{aligned}$$

The active and reactive power flow balances are represented by (2) and (3), respectively. These expressions consider active and reactive power injection at node i by the substation, PV-based DG units, existing

dispatchable DGs, new dispatchable DGs, and MES units to meet the power demand. Note that MES units only participate in the power flow balance with active power injection. According to the operational state of circuits, constraint (5) determines the voltage drop at circuit ij. In this regard, when the operational state of circuit ij is open ($y_{ij,f} = 0$) the slack variable $b^v_{ij,t,c,f}$ is limited according to (5), otherwise, if ($y_{ij,f} = 1$) then $b^v_{ij,t,c,f}$ is equal to zero. Constraint (6) defines the calculation of the square of the current through circuit ij. This conic constraint is linearized in this paper using the piecewise approximation proposed by [24].

The operational constraints of the active devices and operational limits of the system are presented in (7)-(16), where the indices t, c, f correspond to the sets $\Gamma_T, \Gamma^t_C, \Gamma_F$, respectively.

$$0 \leq p^{ss}_{i,t,c,f} \leq \overline{S}^{ss}_i, \qquad \forall(i \in \Gamma_S, t, c, f), \tag{7}$$

$$-\overline{S}^{ss}_i \leq q^{ss}_{i,t,c,f} \leq \overline{S}^{ss}_i, \qquad \forall(i \in \Gamma_S, t, c, f), \tag{8}$$

$$|q_{i,t,c,f}| \leq \sqrt{2}\overline{S}^{ss}_i - p^{ss}_{i,t,c,f}, \qquad \forall(i \in \Gamma_S, t, c, f), \tag{9}$$

$$0 \leq p^{dg}_{i,t,c,f} \leq \overline{P}^{dg}_i, \qquad \forall(i \in \Gamma_G, t, c, f), \tag{10}$$

$$-\overline{S}^{dg}_i \leq q^{dg}_{i,t,c,f} \leq \overline{S}^{dg}_i, \qquad \forall(i \in \Gamma_G, t, c, f), \tag{11}$$

$$|q^{dg}_{i,t,c,f}| \leq \sqrt{2}\overline{S}^{dg}_i - p^{dg}_{i,t,c,f}, \qquad \forall(i \in \Gamma_G, t, c, f), \tag{12}$$

$$0 \leq p^{pv}_{i,t,c,f} \leq P^{pv}_{i,t,c}, \qquad \forall(i \in \Gamma_P, t, c, f), \tag{13}$$

$$|q^{pv}_{i,t,c,f}| \leq p^{pv}_{i,t,c,f} \tan(\arccos(\phi^{pv})), \qquad \forall(i \in \Gamma_P, t, c, f), \tag{14}$$

$$\underline{V}^2 \leq v^{sqr}_{i,t,c,f} \leq \overline{V}^2, \qquad \forall(i \in \Gamma_N, t, c, f), \tag{15}$$

$$\ell^{sqr}_{ij,t,c,f} \leq (\overline{I}_{ij})^2 y_{ij,t,f}, \qquad \forall(ij \in \Gamma_B, t, c, f). \tag{16}$$

Constraints (7)-(9) represent the power capacity of the substations. For existing dispatchable DGs, constraint (10) defines the active power injection limit, while constraints (11) and (12) define the reactive power injection limit. Constraints (13) and (14) define the active and reactive power injection limits of the PV-based generation units, respectively. The voltage and current limits are presented in constraints (15) and (16), respectively.

2.3. Demand response model

This paper explores the advantages of a DR program to improve the restoration process, then the mathematical model that defines a new demand profile of the nodes after each fault event is formulated by (17)-(19). It is worth mentioning that this new demand profile depends on the normal operation demand profile.

$$\sum_{t\in\Gamma_T} p^{dr}_{i,t,c,f}\Delta_t \geq \sum_{t\in\Gamma_T}(P^{d}_{i,t,c}\Delta_t(1-x_{i,t,f})), \qquad \forall(i,c,f), \tag{17}$$

$$P^{d}_{i,t,c}(1-\delta_i)(1-x_{i,t,f}) \leq p^{dr}_{i,t,c,f} \leq P^{d}_{i,t,c}(1+\delta_i)(1-x_{i,t,f}), \qquad \forall(i,t,c,f), \tag{18}$$

$$q^{dr}_{i,t,c,f} = p^{dr}_{i,t,c,f}\tan(\arccos(\mu^{d}_{i})), \qquad \forall(i,t,c,f). \tag{19}$$

Where the indices i,t,c,f correspond to the sets $\Gamma_N,\Gamma_T,\Gamma^t_C,\Gamma_F$, respectively. Constraint (17) requires that the restored energy demand at node i is greater or equal to the energy demanded by that node prior to the fault event. Constraint (18), defines the flexibility of the demand following a pre-fault profile defined by $P^{d}_{i,t,c}$. Finally, constraint (19). determines the reactive power demand at node i during the restoration process according to a constant power factor.

2.4. Dispatching of MES units

In this paper, the DS operator dispatches MES units to improve the recoverability of the system under emergency conditions. These units must be adequately pre-positioned to minimize the travel time from a staging location to a possible DS connection node. The mathematical formulation of this problem is presented in (20)-(32).

$$\sum_{i\in\Gamma^{mes}_N}\sum_{n\in\Gamma^{mes}_{\overline{n}}} z^{mes}_{st,i,n,f} \leq \sum_{n\in\Gamma^{mes}_{\overline{n}}} k^{mes}_{st,n}, \qquad \forall(st,f), \tag{20}$$

$$z^{mes}_{st,i,n,f} \leq z^{mes}_{st,i,n-1,f}, \qquad \forall(st,i,n,f), \tag{21}$$

$$\tau^{x}_{st,i,n,f} = (T^{cf}_{st,i}T^{t}_{st,i} + C^{t}_{i})z^{mes}_{st,i,n,f}, \qquad \forall(st,i,n,f), \tag{22}$$

$$\sum_{t\in\Gamma_T} tw_{i,n,t,f} \geq \sum_{st\in\Gamma_{st}} \tau^{x}_{st,i,n,f}, \qquad \forall(i,n,f), \tag{23}$$

$$\sum_{t\in\Gamma_T} tw_{i,n,t,f} \leq \sum_{st\in\Gamma_{st}} \tau^{x}_{st,i,n,f}+\epsilon, \qquad \forall(i,n,f), \tag{24}$$

$$\sum_{t\in\Gamma_T} w_{i,n,t,f} = \sum_{st\in\Gamma_{st}} z^{mes}_{st,i,n,f}, \qquad \forall(i,n,f), \tag{25}$$

$$u_{i,n,t',f} = \sum_{t\in\Gamma_T} w_{i,n,t,f}, \qquad \forall(i,n,f,t' : t<t'), \tag{26}$$

$$0 \leq p^{mesch}_{i,t,c,f} \leq \overline{P}^{mes} \sum_{n \in \Gamma^{mes}_{\overline{n}}} u_{i,n,t,f}, \qquad \forall (i,n,t,c,f), \tag{27}$$

$$0 \leq p^{mesd}_{i,t,c,f} \leq \overline{P}^{mes} \sum_{n \in \Gamma^{mes}_{\overline{n}}} u_{i,n,t,f}, \qquad \forall (i,n,t,c,f), \tag{28}$$

$$0 \leq soc^{mes}_{i,t,c,f} \leq \overline{SOC}^{mes} \sum_{n \in \Gamma^{mes}_{\overline{n}}} u_{i,n,t,f}, \qquad \forall (i,n,t,c,f), \tag{29}$$

$$soc^{mes}_{i,t,c,f} = soc^{mes}_{i,t-1,c,f} + \eta^{ch}_i \Delta_t p^{mesch}_{i,t,c,f} - 1/\eta^{d}_i \Delta_t p^{mesd}_{i,t,c,f}, \qquad \forall (i,n,t,c,f), \tag{30}$$

$$p^{mesch}_{i,t,c,f} \leq M^{mes} \overline{P}^{mes} e_{i,t,c,f}, \qquad \forall (i,n,t,c,f), \tag{31}$$

$$p^{mesd}_{i,t,c,f} \leq M^{mes} \overline{P}^{mes} (1 - e_{i,t,c,f}), \qquad \forall (i,n,t,c,f). \tag{32}$$

Where the indices st, t, c, n, i, f correspond to the sets $\Gamma_{st}, \Gamma_T, \Gamma^t_C, \Gamma^{mes}_{\overline{n}}, \Gamma^{mes}_N, \Gamma_F$, respectively. Constraint (20) ensures that the number of MES units sent from the staging location st to node i does not exceed the limit of available units at st. Expression (21) defines a sequence for the MES units sent to i. Constraint (22) determines the travel time (τ^x) required by each MES unit from st to i. The travel time is used in (23) and (24) to estimate the connection time of a MES unit at node i. Since the proposed formulation uses a discrete representation of the time, in (24), the parameter ϵ is used to deal with the continuous passage of time between periods. Constraint (25) is used to join the variables that model the MES units sent to new locations, and the binary variables used to estimate the connection time. Constraint (26) guarantees that the MES unit installed at node i remains available for the following periods. Constraints (27) and (28) determine the charging and discharging power of the MES unit installed at node i. Constraint (29) determines the total installed capacity of node i depending on the number of MES units installed. Constraint (30) is used to calculate the state of charge of the MES units installed in the system. Finally, constraints (31) and (32) are used to determine the operational state of the MES units, charge and discharge states, respectively, where M^{mes} is a big number.

2.5. Restoration Problem and Islanding Operation

The proposed restoration approach is based on dynamic switching operations combining grid-connected and islanding operation modes of the existing dispatchable DG units. Then, the solution of the proposed model provides radial network topologies and microgrids for each period and fault scenario.

In this paper, the restoration process aims to disconnect the in-service nodes from the out-of-service nodes of the system. To do so, the mathematical formulation includes a fictitious grid composed of one fictitious substation node that is directly connected to each node of the system through fictitious branches, as proposed in [3]. This fictitious grid connects all the out-of-service nodes of the system during the restoration process.

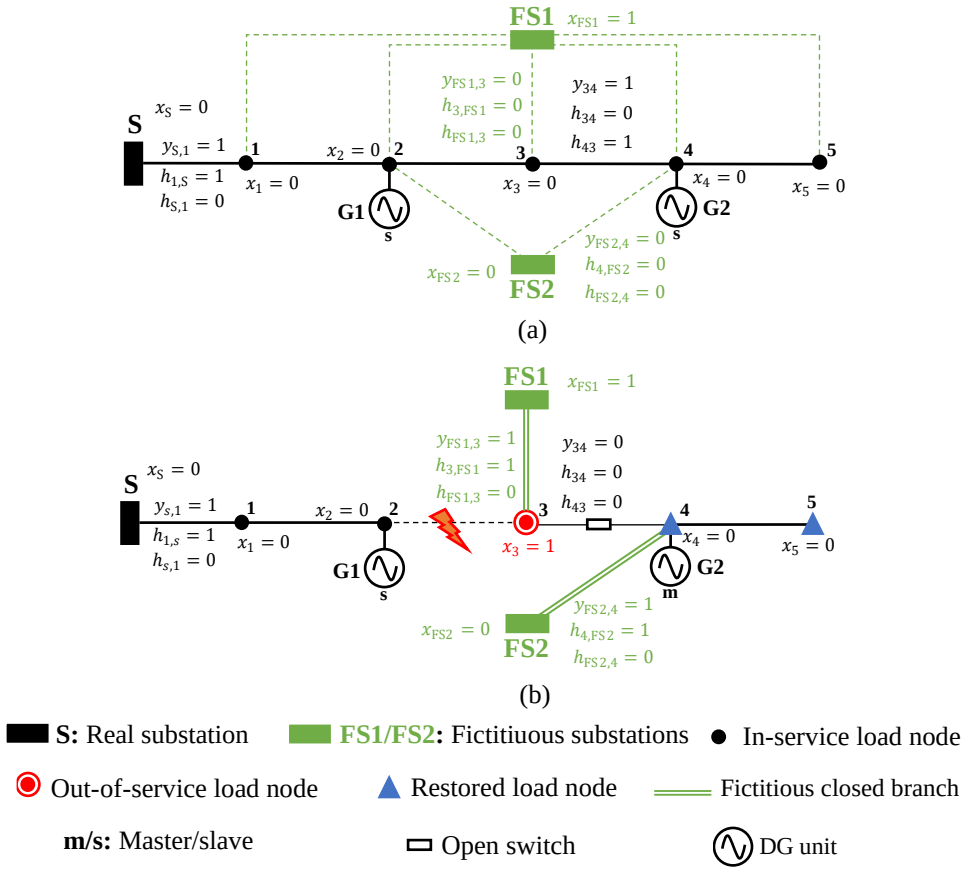

Figure 1: Illustrative six node system for the network topology constraints: (a) Normal operating topology. (b) Emergency topology considering microgrid formation

Regarding the islanding operation mode, nodes with large dispatchable DG installed can be the reference node for a microgrid, while small and renewable power sources operate in slave mode, as proposed in [6]. Then, a second fictitious grid is considered to define the radial microgrid formation and the master/slave status of the DG units. This second grid is composed of one fictitious substation with fictitious branches connected to each node with an existing dispatchable DG capable of operating as a reference node in a microgrid.

Figure 1 illustrates the proposed restoration scheme to determine an emergency topology by network reconfiguration and microgrid formation. Figure 1(a) shows a distribution system with one substation, five load nodes, and two DGs operating in slave mode. The fictitious grid is presented in green with all branches open and two fictitious substations, FS1 and FS2. This figure shows the values for the integer variables h, y, and x for some branches and nodes of the system in normal operating conditions, respectively. Figure 1(b) presents a restored system after applying the proposed restoration scheme by considering a fault scenario involving a permanent fault at branch 2-3 affecting nodes 3, 4, and 5. In the restored system, nodes 4 and 5 were reconnected using a microgrid fed by the DG unit G2 operating as the master unit, while node 3

remains out-of-service. Then it is connected to the fictitious substation FS1 and separated from the main grid by opening switch 3-4. This concept is applied for each period t and fault scenario f.

The set of constraints (33)-(35) represents the radiality of the grid as a spanning tree. This set of constraints aims to maintain the radiality of the in-service part of the system while avoiding the interconnection of substations. Also, these constraints allow for microgrid formation.

$$h_{ij,t,f} + h_{ji,t,f} = y_{ij,t,f}, \qquad \forall (ij \in \Gamma_B \cup \Gamma_B^h, t, f), \tag{33}$$

$$\sum_{ij \in \Gamma_B^*} h_{ij,t,f} = 1, \qquad \forall (i \in \Gamma_N|_{i \notin \Gamma_S}, t, f), \tag{34}$$

$$h_{ij,t,f} = 0, \qquad \forall (ij \in \Gamma_B^*|_{i \in \Gamma_S}, t, f). \tag{35}$$

Where the indices t, f correspond to the sets Γ_T, Γ_F, respectively. The binary variable $y_{ij,t,f}$ determines the operational state of the line ij, in this regard if $y_{ij,t,f} = 0$ the switch at branch ij is open for the fault scenario f, otherwise is closed. Constraint (33) defines the direction of connection between i and j, where the binary variable $h_{ij,t,f}$ determines the direction of the connection between nodes considering the substations nodes as roots of a graph. If $h_{ij,t,f} = 1$, the nodes i and j are connected from j to i at period t and fault scenario f. Constraint (34) ensures that all the nodes of the system are connected by at least one real or fictitious line. To avoid the interconnection of substation nodes, the variable $h_{ij,t,f}$ is set to zero using the constraint (35) as long as i is a substation node.

According to the operational state of the DG units, constraints (36)-(38) define the voltage of these devices. Note that these constraints are related to the second fictitious grid.

$$v_{i,t,c,f}^{sqr} + b_{i,t,c,f}^{g} = (V_i^G)^2, \qquad \forall (i \in \Gamma_G, t, c, f), \tag{36}$$

$$|b_{i,t,c,f}^{g}| = M^v (1 - y_{ij,t,f}), \qquad \forall (ij, t, c, f|_{j \in \Gamma_G \wedge i \in \Gamma_S}), \tag{37}$$

$$y_{ij,t,f} = y_{ij,t-1,f}, \qquad \forall (ij, t, c, f|_{j \in \Gamma_G \wedge i \in \Gamma_S}). \tag{38}$$

Where the indices ij, t, c, f correspond to the sets $\Gamma_B^h, \Gamma_T, \Gamma_C^t, \Gamma_F$. Constraint (36) defines the voltage at nodes with DGs operating as master units. The slack variable $b_{i,t,c,f}^{g}$ is calculated in (37) according to the status of the branch that connects it to the second fictitious substation, where M^v is a big number. If the fictitious branch is closed, then the DG unit at node i will operate as a master unit during the restoration process, the slack variable $b_{i,t,c}^{g}$ is set at 0, and the voltage at node i is fixed at $(V_i^G)^2$. Finally, according to (38), the operational status of the dispatchable DG units must remain the same for the subsequent periods.

The auxiliary constraints (39)-(41) are required to complete the restoration model.

$$|x_{i,t,f} - x_{j,t,f}| \leq (1 - y_{ij,t,f}), \qquad \forall (ij \in \Gamma_B, t, f), \tag{39}$$

$$x_{j,t,f} \geq y_{ij,t,f}, \qquad \forall (ij \in \Gamma_B^h, t, f), \tag{40}$$

$$x_{i,t,f} = 0, \qquad \forall (i \in \Gamma_N^f, t, f). \tag{41}$$

Constraint (39) avoids the connection of out-of-service nodes with in-service nodes, in this constraint, if branch ij is closed ($y_{ij,t,f} = 1$), then $x_{i,t,f} = x_{j,t,f}$, otherwise if branch ij is open ($y_{ij,f} = 0$), then the operational states of nodes, $x_{i,f}$ and $x_{j,f}$, are independent of each other. Constraint (40) is used to ensure that only out-of-service nodes are connected to the fictitious grid. In the proposed approach, for fault scenario f, the nodes that were not affected by this fault must continue to be in-service; thus, constraint (41) sets the load shedding variable $x_{i,f}$ at 0 for the set of in-service nodes Γ_N^f.

2.6. Dispatchable DG allocation constraints

The allocation of dispatchable DG units is considered to enhance the system's recoverability. DG units are modeled to provide backup power and operate as slave units under emergency conditions.

$$0 \leq p_{i,t,c,f}^{ndg} \leq \overline{P}_i^{ndg} g_i, \qquad \forall (i \in \Gamma_G^N, t, c, f), \tag{42}$$

$$\underline{Q}_i^{ndg} g_i \leq q_{i,t,c,f}^{ndg} \leq \overline{Q}_i^{ndg} g_i, \qquad \forall (i \in \Gamma_G^N, t, c, f), \tag{43}$$

$$|q_{i,t,c,f}^{ndg}| \leq \sqrt{2}\overline{P}_i^{ndg} - p_{i,t,c,f}^{ndg}, \qquad \forall (i \in \Gamma_G^N, t, c, f). \tag{44}$$

The set of linear constraints (42)-(44) defines the active and reactive power limits of the new DG units. The binary variable g_i defines the investment decision in new dispatchable DGs in the system, if $g_i = 1$ it is proposed the allocation of a dispatchable DG at note i.

3. Test system and results

The proposed strategy is tested by using the adapted 33-node system from [25] presented in Fig. 2 and the 54-node distribution system with three substations, adapted from [4]. This 54-node system represents a high combinatorial complexity due to the number of substations nodes and the amount of normally-open switches. For both systems, uncertainties in demand and solar irradiation of a typical day are considered through a set of 24 stochastic scenarios with twelve periods of two hours. The scenarios were obtained from historical data of the variables and reduced using the scenario reduction strategy based on k-means presented in [26]. The following test cases are studied to validate the robustness and flexibility of the proposed model

- Case I: The restoration process is based only on switching operations, disregarding the options to dispatch the MES units and the DR program. Additionally, the DG allocation is also disregarded.
- Case II: This case considers the DG allocation while disregarding the MES units and DR program in the restoration process.
- Case III: In this case, the DG allocation is not considered. However, the restoration problem involves all the operational resources.
- Case IV: The DG allocation is used to improve the restoration process considering all the available operational resources.

The proposed approach is based on a MILP formulation that can be solved directly using a commercial optimization solver. Then the optimization model was coded in AMPL and solved using the commercial optimization solver CPLEX 20.1.0, and the numerical experiments were carried out on a computer with a 3.2 GHz Intel® Core™ i7-8100 processor and 32 GB of RAM.

3.1. 33-node system

The 33-node system has two staging locations, as illustrated in Fig. 2, with a capacity of 2 MES units of 0.3 MW and 1.0 MWh, while six nodes are assumed as candidate locations to connect MES units. The system is equipped with three dispatchable DG units of 0.75 MVA and a power factor of 0.8 located at nodes 16, 22, and 29. These units can operate as master DG units. On the other hand, five PV-based DG units of 0.2 MW are located at nodes 5, 7, 13, 21, and 27. The DR program considers that all the nodes can modify their demand up to ± 10% from the pre-fault load state. For planning purposes, nodes 11, 15, 20, 23, and 28 are candidate locations to install the dispatchable DG units, where each unit has a capacity of 0.2 MVA with an investment cost of $10,000 and the load shedding penalty is considered to be 10 $/kWh. Moreover, it is assumed that seven normally-closed automatic switches are installed at branches 1-2, 5-6, 10-11, 14-15, 2-19, 3-23, and 27-28 while five normally-open automatic switches are installed at branches 8-21, 9-15, 12-22, 18-33, and 25-29.

In order to obtain an efficient pre-positioning of MES units and suitable investments in dispatchable DG units, a set of 30 random fault scenarios is assessed. Fig 3 presents the amount of in-service energy demand for each fault scenario. Note that there is no in-service demand at fault scenarios 9, 14, 19, and 28. It is because branch 1-2 is one of the fault branches in these scenarios. For this system, the original power demand of the system is increased by 30% in all demand nodes, so in normal operation, i.e., all the demand nodes are in-service, it is expected that the system has an energy demand of 95.96 MWh during an operational day.

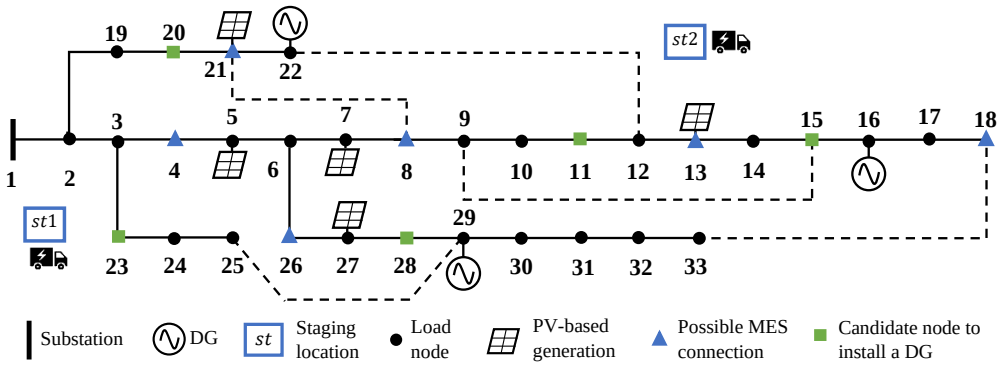

Figure 2: Initial configuration of the 33-node system

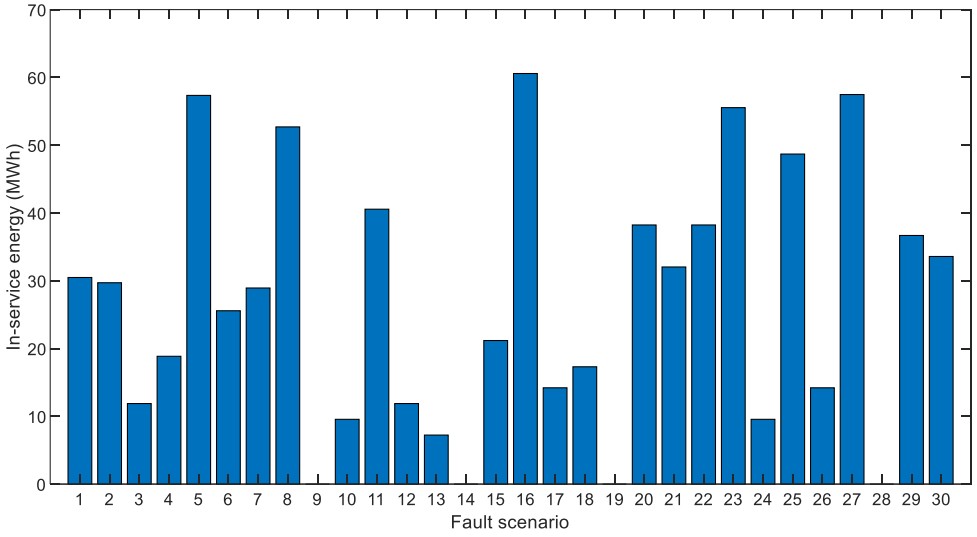

Figure 3: In-service energy for each fault scenarios on the 33-bus system

In this section, fault scenarios 10, 14, and 21 will be analyzed for illustrative purposes. Then, disregarding any corrective action, Table 1 shows the faulted branches, the total disconnected energy demand, the total in-service energy demand, and the in-service nodes.

For case studies I-V and fault scenarios 10, 14, and 21, Table 2 presents the open/closed switches, including the period of the switching operations, and the MES scheduling, including the staging location, connection node, and travel time. It is worth mentioning that MES' travel time considers a continuous-time resolution that does not depend on the periods.

3.1.1. Case I

In fault scenario 10, two microgrids are formed with the DG units at nodes 16 and 22 as master units while the DG unit at node 29 is out of service. The restoration process considers two switching operations at period t_0. In this fault scenario, the in-service energy demand is 30.87 MWh with load at nodes 11, 12, 13, 14, 15, 16, 17, 18, 20, 21, and 22 restored at period t_0 and operating in all the periods. In fault scenario 14,

Table 1: Fault scenarios and their impacts on the 33-bus system

Fault Scen.	Faulted Circuits	Disconn. Demand	In-service Demand	Buses In-service
10	15-16, 3-23, 2-19, 20-19, 5-6, 24-25	86.40 MWh	9.56 MWh	1, 2, 3, 4, 5
14	1-2, 9-10, 13-14, 3-23, 23-24, 30-31	95.96 MWh	0 MWh	1
21	6-26, 5-6, 24-25, 26-27	63.93 MWh	32.03 MWh	1, 2, 3, 4, 5, 19, 20, 21, 22, 23, 24

Table 2: Summary Results of Restoration Process For Cases I–IV

Case	Fault Scen.	Open Circuits	Closed Circuits	MES Dispatch	Nodes for DG Allocation
I	10	[(10-11)t_0]	[(12-22)t_0]	-	
	14	[(2-19)t_0]	[(12-22)t_0]	-	-
	21	[(10-11, 14-15, 27-28)t_0]	[(8-21, 9-15, 18-33)t_0]	-	
II	10	[(10-11, 14-15)t_0]	[(8-21, 9-15, 18-33)t_0]	-	
	14	[(14-15)t_0]	[(8-21, 9-15, 12-22)t_0]	-	11, 15, 20, 28
	21	-	[(8-21, 18-33)t_0]	-	
III	10	[(27-28)t_0; (14-15)t_1]	[(9-15, 12-22, 18-33)t_0; (27-28)t_1]	st1↛13 (4h); st1↛21 (3h); st2↛8 (2h); st2↛18 (2h).	
	14	[(5-6, 14-15, 2-19)t_0]	[(8-21, 9-15, 12-22)t_0; (2-19)t_1; (14-15)t_2]	st1↛4 (2h); st1↛21 (3h); st2↛8 (2h); st2↛18 (2h).	-
	21	[(10-11)t_0]	[(8-21, 12-22, 25-29)t_0; (18-33)t_1]	st1↛13 (4h); st2↛18 (2h); st2↛18 (2h).	
IV	10	[(10-11, 14-15,)t_0]	[(8-21, 9-15, 18-33, 25-29)t_0; (14-15)t_1]	st2↛8 (2h); st2↛8 (2h).	
	14	[(5-6, 10-11, 14-15, 2-19)t_0;]	[(8-21, 9-15, 12-22, 25-29)t_0; (10-11, 2-19)]	st1↛4 (2h); st1↛21 (3h); st2↛8 (2h); st2↛18 (2h).	11, 15, 20, 23, 28
	21	[(10-11)t_0]	[(8-21, 12-22, 18-33, 25-29)t_0]	-	

an in-service energy demand of 25.18 MWh is reached with two switching operations at period t_0 considering that the DG units at nodes 16 and 22 operate as master units. Nodes 10, 11, 12, 13, 14, 15, 16, 17, 18, 19, 20, 21, and 22 are restored at period t_0 and remain in-service in all the periods. In fault scenario 21, six switching operations at period t_0 are proposed to obtain an in-service energy load of 74.65 MWh. The restored system has no microgrids, and nodes 6, 7, 8, 9, 10, 15, 16, 17, 18, 28, 29, 30, 31, 32, and 33 are restored and remain in-service in all the periods. In this case, all the fault scenarios present the switching operations at period t_0, so increasing the number of in-service nodes through periods is impossible.

3.1.2. Case II

The solution of this case defines the allocation of four dispatchable DG units at nodes 11, 20, 28, and 15. In fault scenario 10, the restored system is formed by one microgrid with the dispatchable DG unit at node 29 operating as a master unit, and the in-service energy demand is 62.25 MWh. At period t_0 nodes 6, 7, 8,

9, 10, 15, 16, 17, 18, 20, 21, 22, 26, 27, 28, 29, 30, 31, 32, and 33 are restored and remain in-service through all the periods. On the other hand, the restoration process for fault scenario 14 does not consider microgrids and the in-service load of 57.99 MWh with nodes 2, 3, 4, 5, 6, 7, 8, 9, 10, 11, 12, 13, 15, 16, 17, 18, 19, 20, 21, 22, 26, 27, 28, 29, and 30 in-service in all the periods. In fault scenario 21, the restored system has 83.56 MWh of in-service load. In this case, the restoration process considers all the dispatchable DG units operating as slave units, i.e., the substation node is the reference of the system, and nodes 6, 7, 8, 9, 10, 11, 12, 13, 14, 15, 16, 17, 18, 27, 28, 29, 30, 31, 32, and 33 are restored.

3.1.3. Case III

This case optimizes all the available options, and its solution determines the allocation of five dispatchable DG units at nodes 11, 15, 20, 23, and 28. In addition, two MES units are pre-positioned in each staging location.

Considering the DR program and MES units, the solution presents a more efficient restoration process when compared to Case I. In this case, the pre-positioning of two MES units for each staging location in the system is proposed.

In fault scenario 10, one microgrid is formed with the DG unit located at node 16 operating as a master unit, and the in-service energy of the restored system is 66.81 MWh. The restoration process at period t_0 is composed of four switching operations and two more at period t_1. In this regard, the restored nodes at period t_0 are 16, 17, 18, 28, 29, 30, 31, 32, and 33, while nodes 6, 7, 8, 9, 10, 11, 12, 13, 14, 15, 20, 21, 22, 26, and 27 are restored at period t_1. For this fault scenario, the system requires four MES units at nodes 8, 13, 18, and 21.

By considering fault scenario 14, the restoration process has one microgrid with a DG unit located at node 16 and operating as a master unit. The in-service energy of the restored system is 59.83 MWh. With six switching operations at period t_0 nodes 6, 7, 8, 9, 10, 11, 12, 13, 15, 16, 17, 18, 19, 20, 21, 22, 26, 27, 28, 29, and 30 can be restored. After that, at period t_1, by closing one normally open switch, the set of in-service nodes adds nodes 2, 3, 4, and 5. Finally, by closing one normally open switch, at period t_2, it is possible to restore the load of node 14. In this fault scenario, the MES units are connected at nodes 4, 8, 18, and 21.

In fault scenario 21, four switching operations are required at period t_0 to restore nodes 6, 7, 8, 9, 10, 11, 12, 13, 14, 15, 16, 17, and 18. Later, in period t_1, by closing one normally-open switch, the set of nodes 25, 27, 28, 29, 30, 31, 32, and 33 are included in the set of in-service nodes. Finally, one MES unit is sent to node 13, while two are sent to node 18.

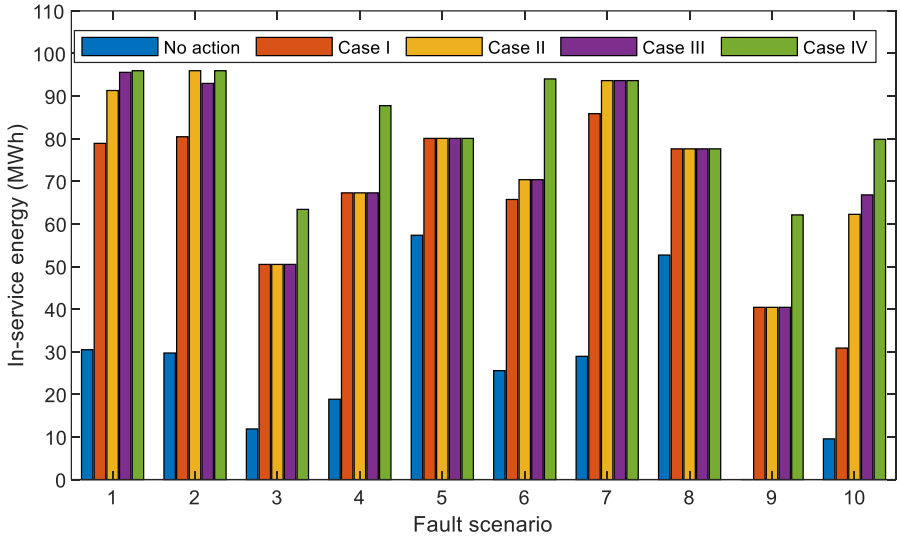

Figure 4: In-service energy for fault scenarios 1-10 for the 33-node system

3.1.4. Case IV

For fault scenario 10, an in-service energy demand of 79.85 MWh is reached by forming one microgrid with node 29 operating as the master DG unit. The solution, at period t_0, proposes six switching operations to restore the set of nodes 6, 7, 8, 9, 10, 15, 16, 17, 18, 20, 21, 22, 25, 26, 27, 28, 29, 30, 31, 32, 33. Later, at period t_1, nodes 11, 12, 13, and 14 are restored by closing one normally-open switch. In this fault scenario, two MES units are connected at node 8. The restoration process for fault scenario 14 determines eight switching operations at period t_0 and two at period t_1 to obtain in-service demand energy of 78.77 MWh. The restored system forms one microgrid with the DG unit at node 22 operating as the master unit. In this case, four MES units are installed in the system, one at nodes 4, 8, 18, and 21. At period t_0, nodes 6, 7, 8, 9, 11, 12, 13, 15, 16, 17, 18, 19, 20, 21, 22, 24, 25, 26, 27, 28, 29, and 30 are restored, and, at period t_1 nodes 2, 3, 4, 5, and 10 are connected to the restored system. Finally, for fault scenario 21, the restored system has no microgrid formation, and all the dispatchable DG units operate as slaves. Considering five switching operations at period t_0, in this case, only node 26 cannot be restored, representing total in-service energy of 94.41 MWh. No MES units are required for this fault scenario.

The results show the advantages of the DG allocation in obtaining a more resilient DS since, in most fault scenarios, it is possible to increase the amount of in-service energy demand compared to cases that disregard the investment in new dispatchable DG units. On the other hand, note that the allocation of dispatchable DG units in the system does not represent an operational issue under normal operational conditions, as these devices can be controlled according to the grid requirements.

By analyzing the in-service energy for each fault scenario presented in Fig. 4 - Fig. 6, the strategy

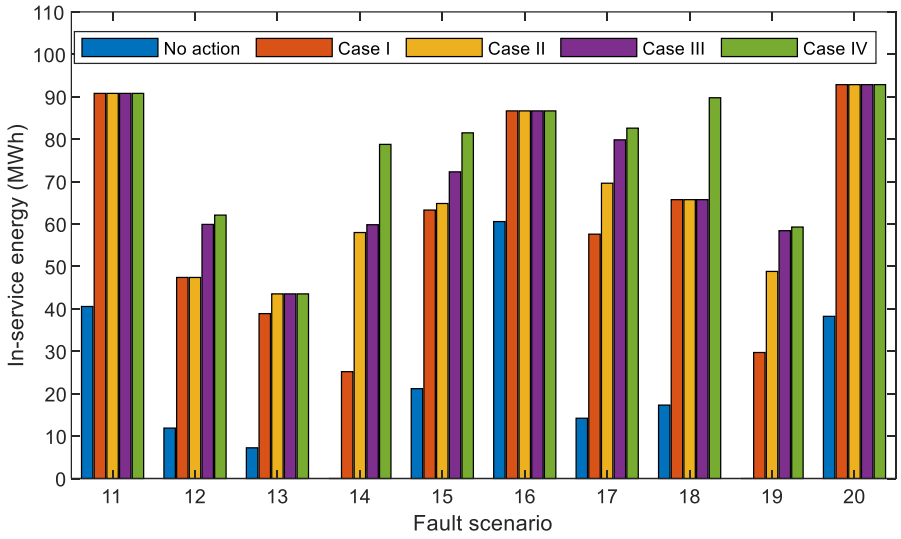

Figure 5: In-service energy for fault scenarios 11-20 for the 33-node system

proposed in study Case IV, considering the DG allocation and operative actions, is the most efficient way to increase the amount of in-service energy of the system. On average, the solution to the problem presents in-service energy of 66.36 MWh, 73.40 MWh, 75.90 MWh, and 82.84 MWh for Cases I-IV, respectively. However, when the DG allocation is disregarded, as presented in the solution of Case I, the system is less resilient, and the in-service energy decreases. Nevertheless, for Case III, the dispatching of MES units and the DR program compensate for the lack of new DG units in the system, increasing the in-service energy of the restored system.

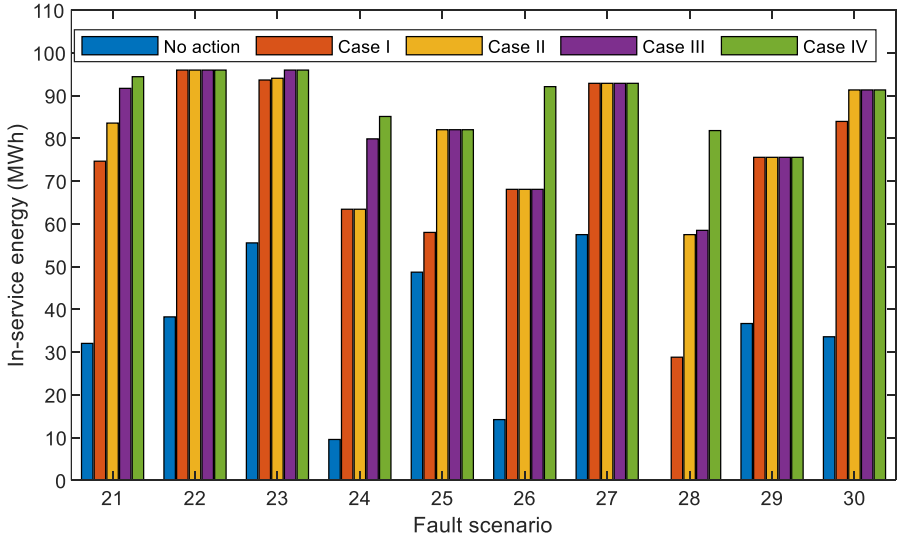

Figure 6: In-service energy for fault scenarios 21-30 for the 33-node system

The problem's solution for fault scenarios 5, 8, 11, 16, 20, 22, 27, and 29 presents the same in-service

Table 3: Summary Results of planning actions for Cases I–IV for the 54-node system

Case	MES pre-positioning	Nodes for DG Allocation	Expected in-service energy [MWh]
I	-	-	730.09
II	-	18, 34, 39, 42, 50	790.40
III	2 MES units at st1 2 MES units at st2	-	793.07
III	2 MES units at st1 2 MES units at st2	22, 13, 18, 39, 42, 50, 34, 46	855.08

energy for Cases I-IV. On the other hand, the problem solution for fault scenarios 7, 13, 25, and 30 presents the same in-service energy for Cases II-IV; however, these cases present a better performance compared to Case I. The most complicated fault scenario was 13 since it is only possible to have in-service energy of 38.87 MWh for Case I, and 43.52 MWh for Cases II-IV. For Case I, the restoration process for fault scenario 13 presents superior performance compared to the restoration process for fault scenarios 14, 19, and 28; notwithstanding, for Cases II-IV, the solution of the problem for fault scenario 13 presents the least amount of energy in service, compared to the other fault scenarios.

These results validate the importance of considering a diverse set of fault scenarios simultaneously to solve the planning part of the problem. This is valid for Cases II-IV. However, in Case I, fault scenarios can be solved independently since there are no common variables among them.

3.2. 53-node system

The 53-node system, shown in Fig. 7, has three substations at nodes 101, 102, and 104 operating at 13.8 kV, two staging locations with a capacity of 3 MES units of 0.3 MW and 1.0 MWh and five nodes are considered as candidate locations to connect MES units. This system has 11 normally open switches represented with dashed lines and 13 normally-closed switches at branches 101-1, 101-3, 4-7, 4-5, 104-30, 37-43, 102-14, 15-16, 102-11, 104-21, 22-9, 38-44, and 42-48. The system has five dispatchable DG units of 3.0 MVA and a power factor of 0.7, capable of operating as master DG units. The entire PV-based generation supplies up to 2 MW to the system. The DR program considers that all the nodes can modify their demand up to $\pm$ 10% from the pre-fault load state. The planning stage considers nodes 7, 13, 18, 22, 34, 39, 42, 46, and 50 as candidate locations to install dispatchable DG units of 0.75 MVA with an investment cost of US$10,000. The load-shedding penalty is 10 US$/kWh. On a typical operational day, the expected energy demand of the system is 998.14 MWh. For this system, a set of 30 random fault scenarios is assessed. Fig 8 presents the amount of in-service energy demand for each fault scenario. Finally, Table 3 presents the main results for each case study

For this test system, Figures 9, 10, and 11 show the expected in-service energy for each fault scenario after the restoration process. Results demonstrate the benefits of considering dispatchable DG allocation to

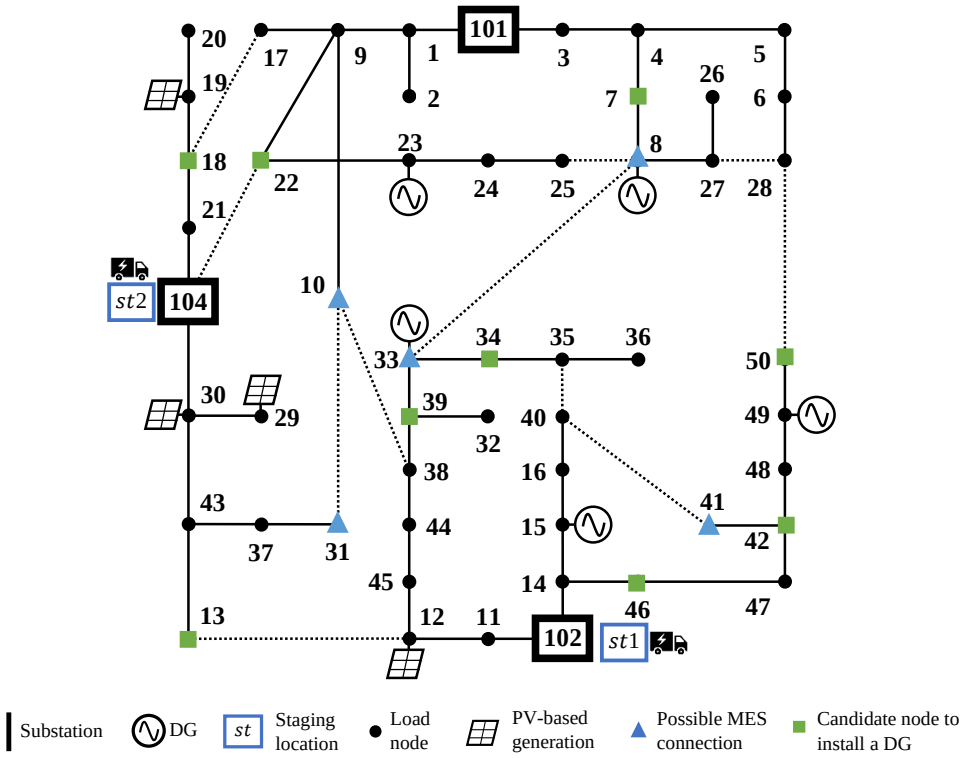

Figure 7: Initial configuration of the 53-node system

increase the amount of in-service energy compared to cases that disregard the investment in these devices. The strategy presented in Case IV is the most effective one for obtaining a resilient DS. In this case, the expected in-service increases energy by 17.12%, 8.18%, and 7.82% compared to Cases I, II, and III, respectively, by pre-positioning four MES units and installing eight DG units. On the other hand, in Case III, combining the optimal dispatch of MES units and the DR program is an effective strategy to improve the restoration process that increments the expected in-service energy by 8.63% and 0.34% compared to cases I and II, respectively. An improvement of 8.26% in the expected in-service energy of Case I is obtained by installing five dispatchable DG units in Case II. However, better results can be achieved by including MES units in the restoration process because MES units are strategically dislocated in each fault scenario to maximize the benefits of these devices.

4. Conclusions

This paper presented a strategy that combines planning and operational alternatives to improve the recoverability of a distribution system. The proposed strategy considers a complete restoration scheme to restore system operation after a set of high-impact fault events, which includes dynamic switching operations, where the in-service part of the system is physically separated from the out-of-service part of the system through radial network reconfiguration and microgrid formation, and the optimal dispatch of MES units.

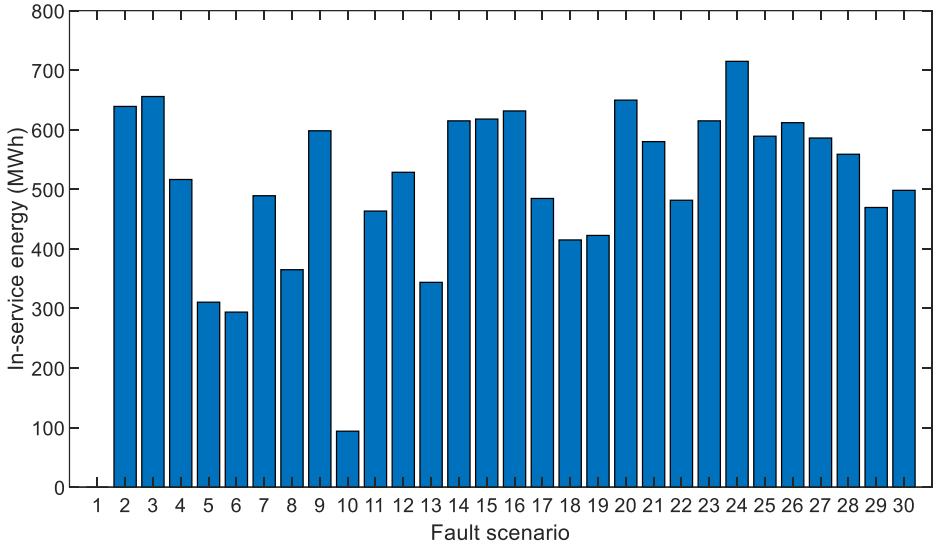

Figure 8: In-service energy for each fault scenarios on the 53-bus system

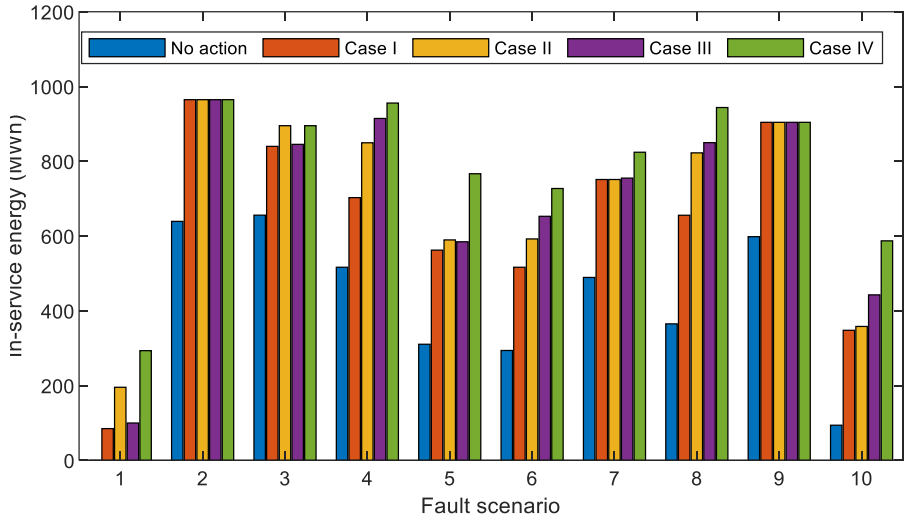

Figure 9: In-service energy for fault scenarios 1-10 for the 53-node system

Additionally, the benefits of applying a demand response program were explored to improve the performance of the restoration process.

Numerical results show the advantages of co-optimizing planning actions and the restoration process to prepare the DS to deal with emergency conditions. From the obtained results, it can be highlighted that by determining the optimal allocation of new dispatchable DG units and the optimal operation of resources such as MES units, the implementation of a DR program, and dynamic reconfiguration, the quantity of in-service load increases more than 10% compared to the solution obtained when only the coordination of switching operations and DG allocation are carried out. It was also determined that when planning and operating actions are co-optimized, the DS has been prepared to deal with emergency conditions in the most efficient way, even though the occurrence of the most complicated fault scenario.

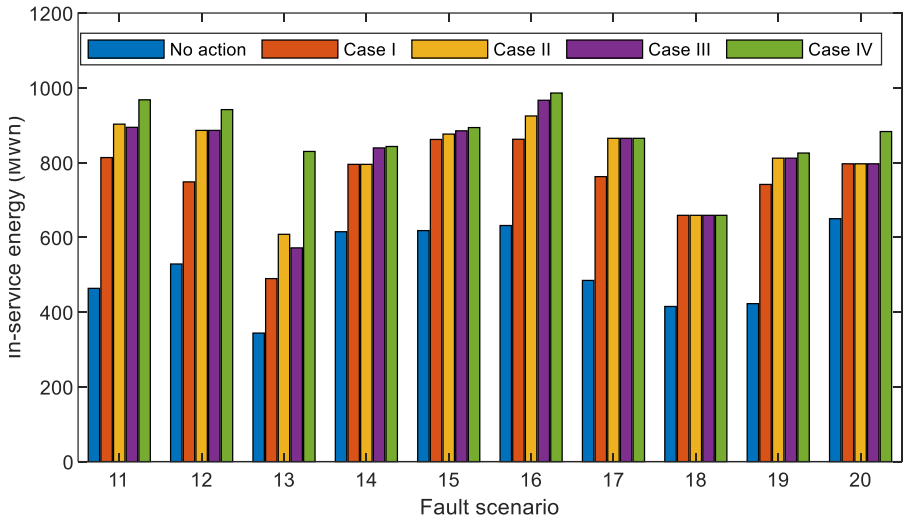

Figure 10: In-service energy for fault scenarios 11-20 for the 53-node system

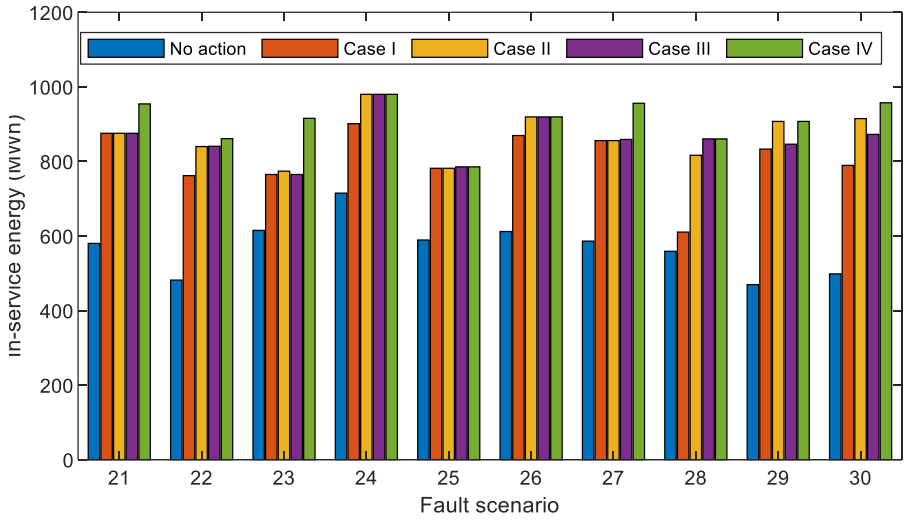

Figure 11: In-service energy for fault scenarios 21-30 for the 53-node system

Future works could address some applications details by including a more suitable representation of demand via a voltage-dependent model and address further advances in the formulation, for example considering a multi-objective framework to estimate the trade-off between investment costs and the amount of energy restored.

Acknowledgment

This paper was supported in part by the São Paulo Research Foundation (FAPESP) under Grants 2019/01841-5, 2019/23755-3, 2018/12422-0 and 2015/21972-6, in part by the Brazilian National Council for Scientific and Technological Development (CNPq) under Grant 304726/2020-6, and in part by the Coor-

dination for the Improvement of Higher Education Personnel (CAPES) finance code 001.

Mohammad S. Javadi acknowledges FCT for his contract funding provided through 2021.01052.CEECIND.

J.P.S. Catalão acknowledges the support by FEDER funds through COMPETE 2020 and by Portuguese funds through FCT, under POCI-01-0145-FEDER-029803 (02/SAICT/2017).

References

[1] F. H. Jufri, V. Widiputra, and J. Jung, "State-of-the-art review on power grid resilience to extreme weather events: Definitions, frameworks, quantitative assessment methodologies, and enhancement strategies," *Applied energy*, vol. 239, pp. 1049–1065, 2019.

[2] D. K. Mishra, M. J. Ghadi, A. Azizivahed, L. Li, and J. Zhang, "A review on resilience studies in active distribution systems," *Renewable and Sustainable Energy Reviews*, vol. 135, p. 110201, 2021.

[3] R. Romero, J. F. Franco, F. B. Leão, M. J. Rider, and E. S. De Souza, "A new mathematical model for the restoration problem in balanced radial distribution systems," *IEEE Transactions on power systems*, vol. 31, no. 2, pp. 1259–1268, 2015.

[4] R. Vargas, L. H. Macedo, J. M. Home-Ortiz, J. R. S. Mantovani, and R. Romero, "Optimal restoration of active distribution systems with voltage control and closed-loop operation," *IEEE Transactions on Smart Grid*, vol. 12, no. 3, pp. 2295–2306, 2021.

[5] Y. Wang, A. O. Rousis, and G. Strbac, "On microgrids and resilience: A comprehensive review on modeling and operational strategies," *Renewable and Sustainable Energy Reviews*, vol. 134, p. 110313, 2020.

[6] T. Ding, Y. Lin, Z. Bie, and C. Chen, "A resilient microgrid formation strategy for load restoration considering master-slave distributed generators and topology reconfiguration," *Applied energy*, vol. 199, pp. 205–216, 2017.

[7] Z. Wang and J. Wang, "Self-healing resilient distribution systems based on sectionalization into microgrids," *IEEE Trans. Power Syst.*, vol. 30, no. 6, pp. 3139–3149, 2015.

[8] B. Chen, C. Chen, J. Wang, and K. L. Butler-Purry, "Multi-time step service restoration for advanced distribution systems and microgrids," *IEEE Trans. Smart Grid*, vol. 9, no. 6, pp. 6793–6805, 2018.

[9] S. Lei, C. Chen, H. Zhou, and Y. Hou, "Routing and scheduling of mobile power sources for distribution system resilience enhancement," *IEEE Transactions on Smart Grid*, vol. 10, no. 5, pp. 5650–5662, 2019.

[10] Y. Xu, Y. Wang, J. He, M. Su, and P. Ni, "Resilience-oriented distribution system restoration considering mobile emergency resource dispatch in transportation system," *IEEE Access*, vol. 7, pp. 73 899–73 912, 2019.

[11] S. Lei, C. Chen, Y. Li, and Y. Hou, "Resilient disaster recovery logistics of distribution systems: Co-optimize service restoration with repair crew and mobile power source dispatch," *IEEE Trans. Smart Grid*, vol. 10, no. 6, pp. 6187–6202, 2019.

[12] B. Taheri, A. Safdarian, M. Moeini-Aghtaie, and M. Lehtonen, "Distribution system resilience enhancement via mobile emergency generators," *IEEE Transactions on Power Delivery*, vol. 36, no. 4, pp. 2308–2319, 2020.

[13] J. Kim and Y. Dvorkin, "Enhancing distribution system resilience with mobile energy storage and microgrids," *IEEE Transactions on Smart Grid*, vol. 10, no. 5, pp. 4996–5006, 2018.

[14] S. Yao, P. Wang, X. Liu, H. Zhang, and T. Zhao, "Rolling optimization of mobile energy storage fleets for resilient service restoration," *IEEE Transactions on Smart Grid*, vol. 11, no. 2, pp. 1030–1043, 2019.

[15] M. R. Kleinberg, K. Miu, and H.-D. Chiang, "Improving service restoration of power distribution systems through load curtailment of in-service customers," *IEEE Transactions on Power Systems*, vol. 26, no. 3, pp. 1110–1117, 2010.

[16] S. Mousavizadeh, M.-R. Haghifam, and M.-H. Shariatkhah, "A linear two-stage method for resiliency analysis in distribution systems considering renewable energy and demand response resources," *Applied energy*, vol. 211, pp. 443–460, 2018.

[17] F. Hafiz, B. Chen, C. Chen, A. R. de Queiroz, and I. Husain, "Utilising demand response for distribution service restoration to achieve grid resiliency against natural disasters," *IET Generation, Transmission & Distribution*, vol. 13, no. 14, pp. 2942–2950, 2019.

[18] J. M. Home-Ortiz, O. D. Melgar-Dominguez, M. S. Javadi, J. Roberto, S. Mantovani, and J. P. Catalão, "Improvement of the distribution systems resilience via operational resources and demand response," *IEEE Transactions on Industry Applications*, vol. 21972, p. 6, 2022.

[19] A. Shahbazi, J. Aghaei, S. Pirouzi, T. Niknam, M. Shafie-khah, and J. P. Catalão, "Effects of resilience-oriented design on distribution networks operation planning," *Electric Power Systems Research*, vol. 191, p. 106902, 2021.

[20] K. S. A. Sedzro, A. J. Lamadrid, and L. F. Zuluaga, "Allocation of resources using a microgrid formation approach for resilient electric grids," *IEEE Trans. Power Systems*, vol. 33, no. 3, pp. 2633–2643, 2018.

[21] J. M. Home-Ortiz and J. R. S. Mantovani, "Resilience enhancing through microgrids formation and distributed generation allocation," in *2020 IEEE PES Innovative Smart Grid Technologies Europe (ISGT-Europe)*. IEEE, 2020, pp. 995–999.

[22] G. Zhang, F. Zhang, X. Zhang, Q. Wu, and K. Meng, "A multi-disaster-scenario distributionally robust planning model for enhancing the resilience of distribution systems," *International Journal of Electrical Power & Energy Systems*, vol. 122, p. 106161, 2020.

[23] J. M. Home-Ortiz, O. D. Melgar-Dominguez, J. R. S. Mantovani, and J. P. Catalão, "Pv hosting capacity assessment in distribution systems considering resilience enhancement," *Sustainable Energy, Grids and Networks*, p. 100829, 2022.

[24] N. Alguacil, A. L. Motto, and A. J. Conejo, "Transmission expansion planning: a mixed-integer lp approach," *IEEE Transactions on Power Systems*, vol. 18, no. 3, pp. 1070–1077, 2003.

[25] M. E. Baran and F. F. Wu, "Network reconfiguration in distribution systems for loss reduction and load balancing," *IEEE Power Engineering Review*, vol. 9, no. 4, pp. 101–102, 1989.

[26] J. M. Home-Ortiz and J. R. S. Mantovani, "Enhancement of the resilience through microgrids formation and dg allocation with master-slave dg operation," in *2020 International Conference on Smart Energy Systems and Technologies (SEST)*. IEEE, 2020, pp. 1–6.